

Original Article



# Distinct Transcriptional and Functional Differences of Lung Resident and Monocyte-Derived Alveolar Macrophages During the Recovery Period of Acute Lung Injury

Fei Hou <sup>1,2,†</sup>, Huan Wang <sup>3,†</sup>, Kun Zheng <sup>3</sup>, Wenting Yang <sup>3</sup>, Kun Xiao <sup>1</sup>, Zihan Rong <sup>4</sup>, Junjie Xiao <sup>1,2</sup>, Jing Li <sup>3</sup>, Baihe Cheng <sup>3</sup>, Li Tang <sup>3,\*</sup>, Lixin Xie <sup>1,\*</sup>

OPEN ACCESS

**Received:** Nov 22, 2022  
**Revised:** Jan 18, 2023  
**Accepted:** Feb 27, 2023  
**Published online:** Mar 23, 2023

**\*Correspondence to**

Lixin Xie

College of Pulmonary & Critical Care Medicine, 8th Medical Center, Chinese PLA General Hospital, 28th Fuxin Road, Beijing 100853, China.  
Email: xielx301@126.com

Li Tang

State Key Laboratory of Proteomics, National Center for Protein Sciences and Beijing Proteome Research Center, Beijing Institute of Lifeomics, 38 Life Science Park Road, Changping District, Beijing 102206, China.  
Email: tangli@ncpsb.org.cn

<sup>†</sup>Fei Hou and Huan Wang contribute equally to this work.

Copyright © 2023. The Korean Association of Immunologists

This is an Open Access article distributed under the terms of the Creative Commons Attribution Non-Commercial License (<https://creativecommons.org/licenses/by-nc/4.0/>) which permits unrestricted non-commercial use, distribution, and reproduction in any medium, provided the original work is properly cited.

**ORCID iDs**

Fei Hou   
<https://orcid.org/0000-0003-1928-072X>  
Huan Wang   
<https://orcid.org/0009-0008-6673-3721>

<sup>1</sup>College of Pulmonary & Critical Care Medicine, 8th Medical Center, Chinese PLA General Hospital, Beijing, China

<sup>2</sup>Medical School of Chinese PLA, Beijing, China

<sup>3</sup>State Key Laboratory of Proteomics, National Center for Protein Sciences, Beijing Proteome Research Center, Beijing Institute of Lifeomics, Beijing, China

<sup>4</sup>College of Life Sciences, Hebei University, Baoding, China

## ABSTRACT

In acute lung injury, two subsets of lung macrophages exist in the alveoli: tissue-resident alveolar macrophages (AMs) and monocyte-derived alveolar macrophages (MDMs). However, it is unclear whether these 2 subsets of macrophages have different functions and characteristics during the recovery phase. RNA-sequencing of AMs and MDMs from the recovery period of LPS-induced lung injury mice revealed their differences in proliferation, cell death, phagocytosis, inflammation and tissue repair. Using flow cytometry, we found that AMs showed a higher ability to proliferate, whereas MDMs expressed a larger amount of cell death. We also compared the ability of phagocytosing apoptotic cells and activating adaptive immunity and found that AMs have a stronger ability to phagocytose, while MDMs are the cells that activate lymphocytes during the resolving phase. By testing surface markers, we found that MDMs were more prone to the M1 phenotype, but expressed a higher level of pro-repairing genes. Finally, analysis of a publicly available set of single-cell RNA-sequencing data on bronchoalveolar lavage cells from patients with SARS-CoV-2 infection validated the double-sided role of MDMs. Blockade of inflammatory MDM recruitment using CCR2<sup>-/-</sup> mice effectively attenuates lung injury. Therefore, AMs and MDMs exhibited large differences during recovery. AMs are long-lived M2-like tissue-resident macrophages that have a strong ability to proliferate and phagocytose. MDMs are a paradoxical group of macrophages that promote the repair of tissue damage despite being strongly pro-inflammatory early in infection, and they may undergo cell death as inflammation fades. Preventing the massive recruitment of inflammatory MDMs or promoting their transition to pro-repairing phenotype may be a new direction for the treatment of acute lung injury.

**Keywords:** Alveolar Macrophage; Monocyte-Derived Macrophage; Acute Lung Injury; Inflammation

Kun Zheng 


<https://orcid.org/0000-0003-3379-3003>

Wenting Yang 

<https://orcid.org/0009-0000-0684-5176>

Kun Xiao 

<https://orcid.org/0000-0002-8039-3283>

Zihan Rong 


<https://orcid.org/0009-0007-4665-0454>

Junjie Xiao 

<https://orcid.org/0009-0001-0418-8448>

Jing Li 

<https://orcid.org/0009-0000-6945-6776>

Baihe Cheng 

<https://orcid.org/0000-0002-1545-0528>

Li Tang 

<https://orcid.org/0000-0001-5368-490X>

Lixin Xie 

<https://orcid.org/0000-0002-1091-2041>

### Conflict of Interest

The authors declare no potential conflicts of interest.

### Abbreviations

7-AAD, 7-aminoactinomycin D; ALI, acute lung injury; AM, alveolar macrophage; BALF, bronchoalveolar lavage fluid; CFSE, carboxyfluorescein succinimidyl ester; DEG, differentially expressed gene; GEO, Gene Expression Omnibus; GO, Gene Ontology; GSEA, gene set enrichment analysis; i.p., intraperitoneal; i.t., intratracheal; iMDM, inflammatory monocyte-derived alveolar macrophage; KEGG, Kyoto Encyclopedia of Genes and Genomes; MDM, monocyte-derived alveolar macrophage; PCA, principal component analysis; pMDM, pro-repairing monocyte-derived alveolar macrophage; RELM- $\alpha$ , resistin-like molecule  $\alpha$ ; RNA-seq, RNA-sequencing; scRNA-seq, single-cell RNA-sequencing; WT, wild-type

### Author Contributions

Conceptualization: Hou F, Wang H, Yang W, Tang L, Xie L; Data curation: Wang H, Zheng Kun, Xiao K, Xiao J; Formal analysis: Hou F, Rong Z; Investigation: Hou F, Yang W; Methodology: Zheng K; Project administration: Xiao K; Software: Li J; Supervision: Tang L, Xie L; Validation: Cheng B; Writing - original draft: Hou F, Wang H, Zheng K, Xiao J; Writing - review & editing: Yang W, Xiao K, Rong Z, Li J, Tang L, Xie L.

## INTRODUCTION

Acute lung injury (ALI) is characterized by diffuse alveolar damage and a lack of effective treatments (1). Alveolar macrophages (AMs) and monocyte-derived macrophages (MDMs) are two subsets of lung macrophages that exist in the injured lung and take part in the whole process of ALI, including pathogenesis and resolution (2-4). AMs are tissue-resident macrophages that reside in alveolar cavities. They originate from the yolk sac and fetal liver and are the first sentinels to defend against pathogens and dust (5-8). MDMs are recruited macrophages that enter alveoli during infection or injury. AMs and MDMs are all believed to be important mediators of ALI recovery (9,10). They transit from the so-called M1 to M2 phenotypes and are involved in apoptotic cell phagocytosis and tissue injury repair (11,12). However, whether they have the same phenotype and function remains unclear, making it difficult to target macrophages to intervene in the lung injury process.

RNA-sequencing (RNA-seq) revealed significant differences between AMs and MDMs at the transcriptional level, especially in proliferation, metabolism, phagocytosis, cell death, cytokine release, and pro-repairing functions. We compared the proliferation ability, cell death level, phagocytic ability, phenotype, and pro-repair function of AMs and MDMs during the recovery period of ALI. AMs have a high proliferation rate and strong phagocytic ability with a repressed phenotype and stronger vitality. Whereas, MDMs have shown paradoxical characteristics. MDMs are short-lived cells that show high expression of inflammatory markers compared to AMs, but release a higher level of growth factors that help repair the injured tissue. The presence of a large number of inflammatory MDMs (iMDMs) is an important reason for the aggravation of lung injury, and timely resolution of inflammatory MDMs or conversion to a pro-repairing phenotype can help the recovery of infection and injury.

## MATERIALS AND METHODS

### Patients data

Public data set (Gene Expression Omnibus [GEO]: GSE145926) which contain single-cell RNA-seq (scRNA-seq) data from bronchoalveolar lavage fluid (BALF) cells from 3 patients with moderate COVID-19 (M1-M3), 6 patients with severe/critical COVID-19 (S1-S6), 3 healthy controls (HC1-HC3) were used for bioinformatic analysis. Ethical approval was obtained from the Research Ethics Committee of 8th Medical Center, Chinese PLA General Hospital (202205311004).

### Mice

C57BL/6 wild-type (WT) mice were purchased from Charles River in Beijing (Vital River). *Ccr2*<sup>-/-</sup> (B6.129S4-Ccr2tm1Ifc/J) mice were purchased from Jackson Laboratory. All mice (8 weeks old) were housed in a pathogen-free facility of the Beijing Institute of Lifeomics. All experiments were conducted under protocols approved by the Animal Care and Use Committee (IACUC-20200221-02M).

### Mouse preparation

Mice were anesthetized (2.5% avertin, 20 ml/kg, intraperitoneal [i.p.]; MilliporeSigma, Saint Louis, MO, USA) before LPS instillation. *Escherichia coli* LPS (O111:B4 Sigma-Aldrich L2630) at 2  $\mu$ g/g mouse or PBS as control was instilled intratracheally [i.t.] via a 24-gauge catheter. On 1, 3, 5, and 7 days after instillation, mice were anesthetized and killed by exsanguinations

from their inferior vena cava. In some experiments, mice were anesthetized and killed 6 days after instillation.

### Analysis of BALF

BAL was obtained by cannulating the trachea with a 20-gauge catheter. The right lung was lavaged three times with a single inoculum of 600  $\mu$ l sterile PBS. BAL was then centrifuged at 500 g for 5 min at 4°C. Supernatants were stored at -80°C for later analysis. The cell pellet was diluted in PBS with 2 Mm EDTA and then performed for flow cytometry (as described below). Total protein was measured in the cell-free supernatant using the method of bicinchoninic acid.

### Wet/dry ratio

The left lobe of the lung was resected after LPS-induced injury, weighed and dried at 55°C for 24 h to calculate the lung wet to dry ratio.

### Flow cytometry and cell sorting

Cells were incubated with Fc Block-2.4G2 (70-0161) Ab to block Fc $\gamma$  III/II receptors before staining with a specific Ab. For surface marker analysis, cell pellets were stained with the appropriate Abs at 4°C for 20–30 min. For intracellular cytokine analysis, cells were stained with the Cytofix/Cytoperm kit according to the manufacturer's instructions (eBioscience, San Diego, CA, USA). The following Abs were used for staining: CD45-AF700 (30-F11), Ly6G-PEcy7 (1A8), CD64-APC (X54-5/7.1), MerTK-BV711 (DS5MMER), Siglec-F-BV421 (E50-2440), CD11b-BV510 (M1/70), CD206-PE (C068C2), CD86-FITC (GL-1) RELM alpha-PerCP-eFluor™ 710 (DS8RELM), Ki67-eFluor™ 660 (SolA15), CD3-BV421 (17A2), CD44-FITC (1M7), CD25-FITC (7D4), CD69-PE (H1.2F3). Flow cytometry was performed using an LSR II Fortessa (BD Biosciences, San Jose, CA, USA). The acquired data were analyzed with FlowJo software (Tree Star). For cell sorting, a FACS Aria III (BD Biosciences) was used.

### RNA-seq

The 10<sup>6</sup> AMs or MDMs of each sample were sorted from 5 ALI mice on day 6. The RNA sequencing was completed in Annoroad Gene Technology Corporation (Beijing, China). RNA samples were sequenced using Illumina NovaSeq 6000 according to the standard protocol. Raw data were filtered to obtain clean data. Analysis were conducted using the clean data. Reads were mapped to the mouse genome GRCh38 with HISAT2 and were quantified with the featureCounts function.

### RNA-seq data analysis

The DEGs between AMs and MDMs were calculated by the DESeq2 package, then screened with FDR <0.05 and  $|\log_2FC| > 1$  to identify the differences. Furthermore, Gene Ontology (GO) function and Kyoto Encyclopedia of Genes and Genomes (KEGG) functional enrichment analysis was performed using the ClusterProfiler (V3.16.1) package. The gene set enrichment analysis (GSEA) were conducted by clusterProfiler R package and visualized by the ggplot2 R package (R Project for Statistical Computing, Vienna, Austria).

### EdU staining

Mice were administrated 0.5 mg EdU (Thermo Fisher Scientific, Waltham, MA, USA) via i.p. injection. After 24 h, BALF cells were obtained and EdU incorporation was measured by flow cytometry using the Click-iT EdU Alexa Fluor 647 Flow Cytometry Assay Kit (Thermo Fisher Scientific) according to the manufacturer's instructions.

### Phagocytosis analysis

Thymus was obtained from three-week-old mice and then labeled with carboxyfluorescein succinimidyl ester (CFSE), after which cells were killed at 65°C for 10 min. Heat-killed cells were injected into the lungs of lung-injured mice by tracheal injection, and flow cytometry was performed 1 h later.

### T cell activation assay

CD3<sup>+</sup> CD44<sup>-</sup> Naïve T cells were sorted from mouse lymph nodes and seeded into CD3-coated (BD Clone: 145-2C11) 48-well plates ( $5 \times 10^5$ /well). Naïve T cells were cultured in RPMI 1640 supplemented with 10% FBS and CD28-Ab (TONBO Clone: 37.51) for 8 h. Afterwards, T cells were co-cultured overnight with AMs or MDMs. Activated T cells were then harvested for flow cytometry analysis.

### Cell migration assay

Macrophages were seeded in 24-well plates ( $1 \times 10^6$ /well), and after adhesion, linear scratch were made in the cell monolayers with a 200- $\mu$ l pipette tip. The area of scratch wound was measured by using ImageJ software 0, 6, 12, 24 h after stimulation.

### Single-cell data analysis

scRNA-seq data GSE145926 including 3 patients with moderate COVID-19 (M1–M3), 6 patients with severe/critical infection (S1–S6), 3 healthy controls (HC1–HC3) and a publicly available BALF (HC4) sample were download from GEO databases. Macrophages were re-integrated and re-clustered from the nCoV.rds, The data was first normalized using ‘LogNormalize’ methods in Seurat (v.3.1.0) with default parameters. The top 2,000 variable genes were then identified using the ‘vst’ method in Seurat FindVariableFeatures function and the FindCluster package used for cell cluster analysis with the resolution set to 0.8.

### Histopathological analysis

Lungs were inflated and fixed for 48 hours with 10% formalin, and then embedded in paraffin. 5  $\mu$ m sections were cut and stained with H&E, Slides were scanned and pictures were taken using Leica Aperio slide scanner (Leica, Wetzlar, Germany).

### Statistical analyses

Statistical analysis was performed with GraphPad Prism v8 software. Data are presented as mean $\pm$ SEM. Sample data with normal distribution were analyzed using Student’s t-test or one-way ANOVA where appropriate.

## RESULTS

### AM and MDM dynamics in LPS-induced lung injury model

The classical LPS tracheal injection-induced lung injury model was used, and a gating strategy to differentiate AMs and MDMs was adopted based on the differential expression levels of Siglec F and CD11b in AMs and MDMs (**Fig. 1A**) (4,13,14). Intratracheal instillation of LPS resulted in tissue damage and inflammation. The peak of inflammation and tissue injury occurred on day 3 and resolved on day 5 (**Fig. 1B–D**). AM numbers first declined during the acute inflammatory response phase and gradually recovered during the recovery period, whereas MDMs were recruited early and then declined (**Fig. 1E**). The dynamics of AMs and

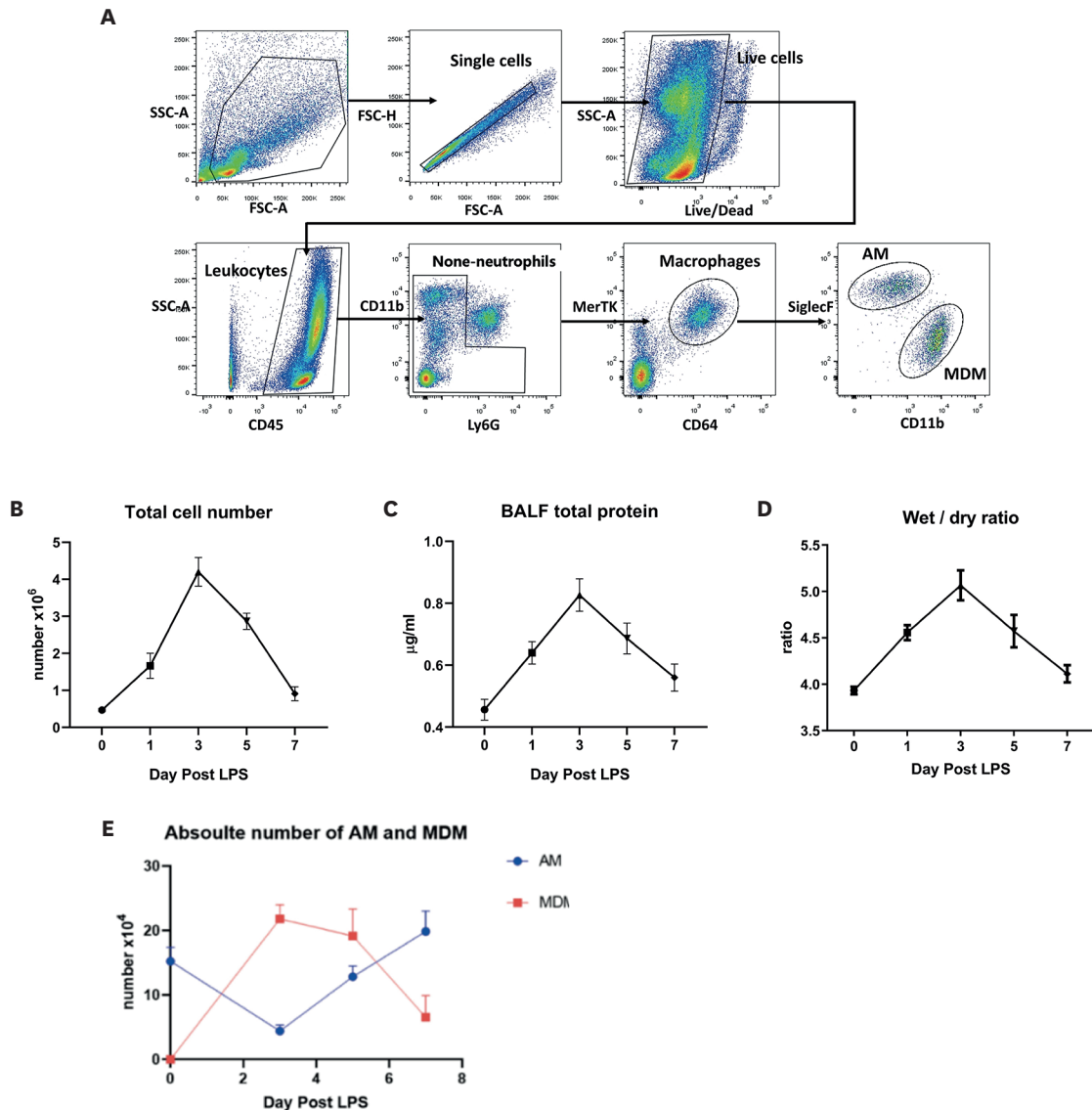


**Figure 1.** AMs and MDMs in LPS-induced ALI. (A) Gating strategy of AMs and MDMs in BALF cells. AMs were identified as CD45<sup>+</sup>Ly6G<sup>-</sup>CD64<sup>+</sup>MerTK<sup>+</sup>SiglecF<sup>+</sup>CD11b<sup>-</sup> cells; MDMs were identified as CD45<sup>+</sup>Ly6G<sup>-</sup>CD64<sup>-</sup>MerTK<sup>-</sup>SiglecF<sup>-</sup>CD11b<sup>+</sup> cells. (B, C) Total cell number and protein level dynamics in ALI mice BALF (n=3 per time point). (D) Wet/dry weight ratio changes of lung tissue in ALI mice. (E) Dynamic changes of AMs and MDMs in mice BALF (n=3 per time point).

MDMs were contrasting, and they reached a similar quantity on day 6. Therefore, day 6 was chosen as the time point for analyzing AMs and MDMs.

### Transcriptional differences between AMs and MDMs during the recovery period

AMs and MDMs from day 6 in ALI mice were sorted for RNA-seq (Fig. 2A). Principal component analysis (PCA) and cluster dendrograms revealed obvious differences in AMs and MDMs (Fig. 2B, Supplementary Fig. 1). A total of 2,732 differentially expressed genes (DEGs) between AMs and MDMs were identified, of which 1,212 genes were downregulated and 1,520 were upregulated as displayed in a volcano plot (Fig. 2C). Some genes representing inflammation, repairing and cell death, such as *Nos2*, *IL6*, *Ccl5*, *Pdgra* and *Bcl2*, were significantly up-regulated in MDMs. While AMs up-regulated *Mrc1*, *Ccna2*, *Ccnd2*, *Marco*, *Cd209b* and *SiglecF*, which were related to cell proliferation and phagocytosis (Fig. 2C). The

heatmap of top 50 DEGs was also made to show gene expression differences between AMs and MDMs (Fig. 2D). Next, the GO and KEGG pathways were analyzed. GO analysis revealed that MDMs are mainly involved in leukocyte migration, cell chemotaxis, and cytokine production, whereas AMs are involved in nuclear division and the cell cycle (Fig. 3A and B). KEGG pathway enrichment showed that AMs enriched pathways related to cell cycle, fatty acid metabolism, and DNA replication whereas MDMs enriched cell adhesion and immune signaling pathways (Fig. 3C). These results indicate that AMs are in a state of strong cell proliferation and have a higher levels of fatty acid metabolism, whereas MDMs retain the chemotactic characteristics of monocytes and secrete more cytokines. Partially consistent with the GO and KEGG analyses results, AMs and MDMs showed large differences in genes that represent functions of phagocytosis, proliferation, inflammation, and cell death (Fig. 3D).

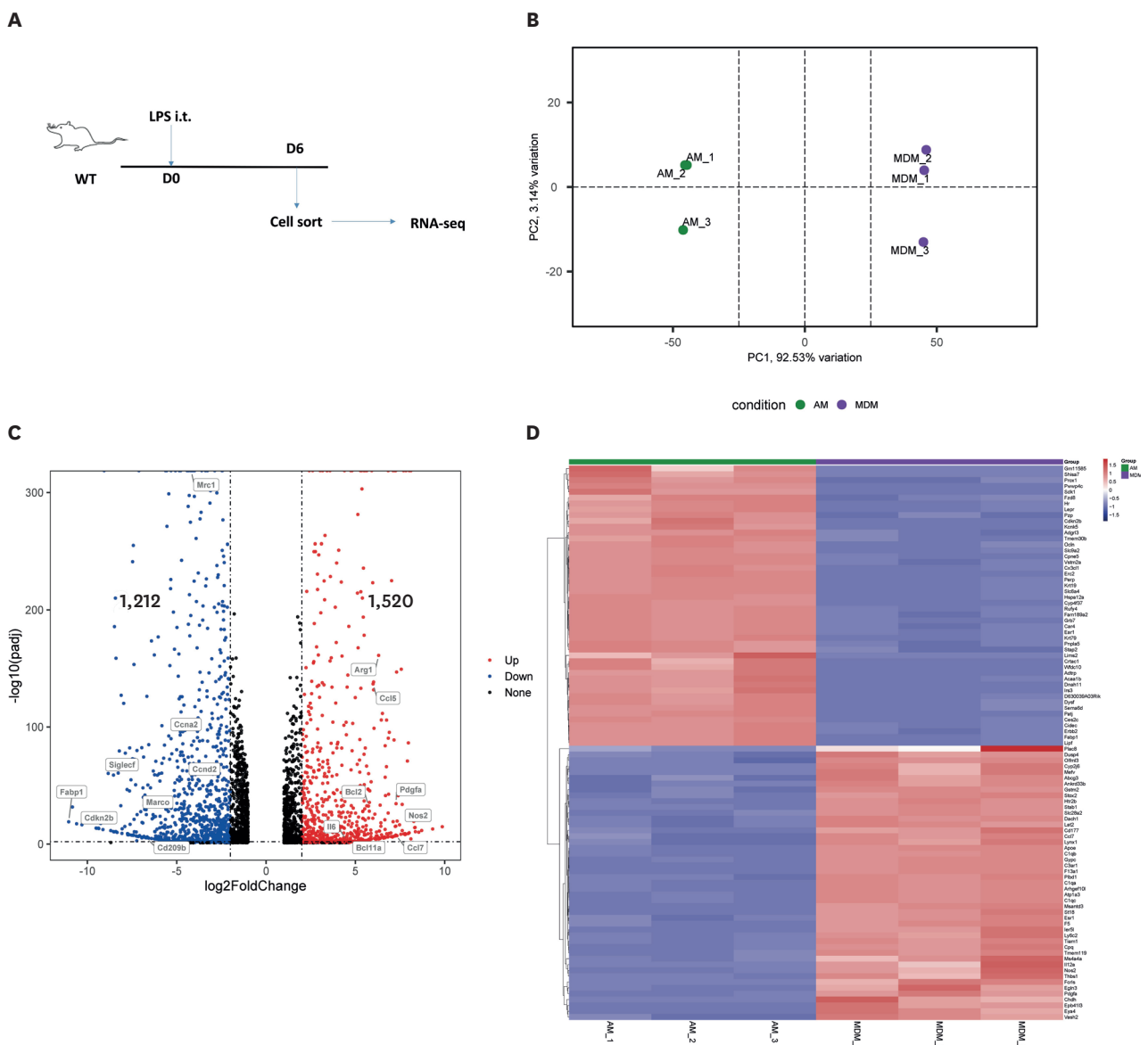


**Figure 2.** Gene expression differences between AMs and MDMs. (A) Experiment design for sorting and sequencing of AMs and MDMs. (B) PCA of AMs and MDMs that sorted from ALI mice BALF on day 6 (each point represents 5 mice). (C) Volcano plot of differentially expressed genes in AMs and MDMs. (D) Clustering heatmap of the top 50 differentially expressed genes in AMs and MDMs.

Differences of Alveolar Macrophages

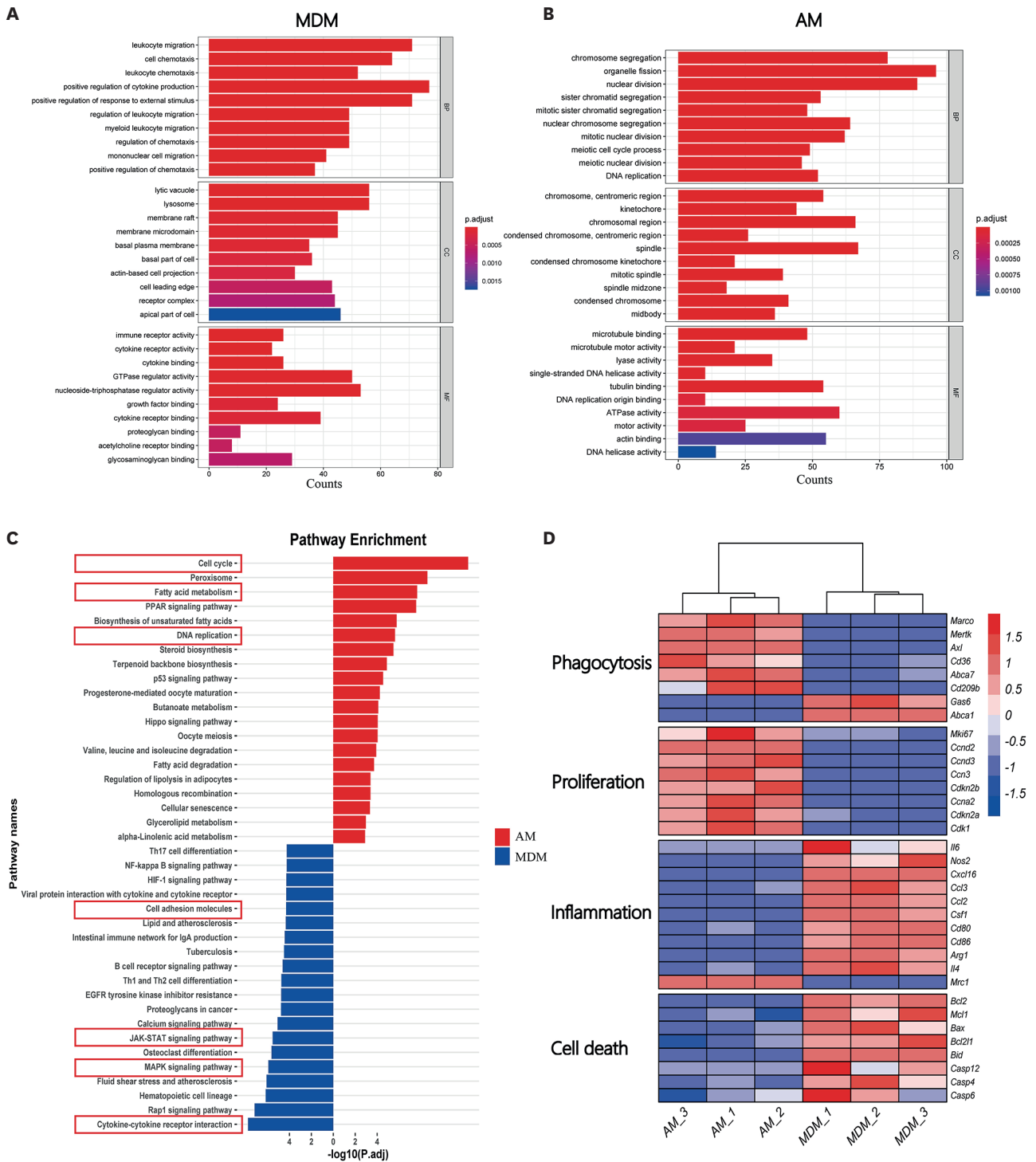


**Figure 3.** Transcriptional level differences between AMs and MDMs. (A, B) Top 10 BP, CC, and MF enrichments of MDMs and AMs that sorted from ALI mice BALF on day 6. (C) Top 20 upregulated and downregulated KEGG pathways of MDMs that sorted from ALI mice BALF on day 6. (D) Heatmap of genes that represent phagocytosis, proliferation, inflammation, and cell death of AMs and MDMs that sorted from ALI mice BALF on day 6. BP, biological function; CC, cellular component; MF, molecular function.

### AMs have stronger viability and phagocytic ability compared with MDMs

Studies have shown that AMs are self-renewing macrophages that can repopulate their numbers independent of MDM supplements (15,16). DEGs also showed that AMs expressed stronger cell cycle-related genes. Therefore, we compared the proliferative abilities of AMs and MDMs using Ki67 and EDU staining. At day 6 of lung injury, AMs showed a stronger ability to proliferate, whereas MDMs exhibited low proliferation (Fig. 4A and B). The cell death levels of AMs and MDMs were also analyzed. As expected, MDMs showed higher levels of cell death *in vivo*, as indicated by the percentage of 7-aminoactinomycin D (7-AAD)+ cells (Fig. 4C).

Phagocytosis of apoptotic cells, an important function of macrophages, contributes to timely resolution of inflammation (12). However, the role of macrophages in phagocytosis of apoptotic cells remains controversial. To explore the phagocytic function of AMs and MDMs, CFSE-labeled apoptotic thymocytes were injected *i.t.* 6 days post LPS stimulation to investigate the phagocytic function of AMs and MDMs (Fig. 4D). The proportion of CFSE+AMs was significantly higher than that of CFSE+MDMs, indicating that AMs may have a stronger ability to phagocytize apoptotic cells (Fig. 4E).

### MDMs have strong adhesion ability and promote lymphocyte differentiation and activation

Macrophage functions, such as tissue repair and phagocytosis, are related to cell adhesion and motility. One study showed that AMs move towards inhaled bacteria within the alveoli and that macrophage migration is crucial for bacterial clearance (17). MDMs exhibited stronger cell adhesion and motility abilities, according to the GSEA results (Fig. 4F).

Macrophages are also important cells that connect the innate and adaptive immunities. They control the initiation of adaptive immunity via Ag presentation and lymphocyte activation. Lymphocyte activation, proliferation, and differentiation are critical processes in the adaptive immunity. The ability to promote adaptive immune activation was compared and found that MDMs, rather than AMs, promoted lymphocyte activation, proliferation, and differentiation (Fig. 4F). To verify GSEA results, AMs and MDMs from day 6 in ALI mice were sorted and co-cultured with CD3/CD28-activated T cells. T cells from MDM-T co-culture system expressed stronger T cell activation markers CD25 and CD69 (Fig. 4G), which means MDMs may have stronger ability in activating lymphocytes. An *in vitro* scratch-wound healing assay was also made to study cell migration difference of AMs and MDMs. Consistent with the results of GSEA, MDMs showed enhanced ability of migration at 12 and 24 h after the scratch (Fig. 4H).

### MDMs are prone to “M1” phenotype but express a high level of pro-repairing genes

Macrophages undergo phenotypic transition and promote the resolving of inflammation and repairing of tissue injury during the recovery phase (18,19). The expression of M1 and M2 markers of AMs and MDMs were compared and found that AMs expressed higher levels of CD206 and resistin-like molecule  $\alpha$  (RELM- $\alpha$ ), which are both M2 markers, whereas MDMs expressed higher levels of M1 marker CD86 and inducible nitric oxide synthase (Fig. 5A). Consistent with the M1 phenotype, MDMs were more inflammatory and produced more cytokines according to the GSEA (Fig. 5B). A high expression of M2 markers usually indicates a high ability to promote tissue repair. MDMs, which were prone to the M1 phenotype, expressed higher levels of pro-repairing genes, such as Vegfa, Pdgfa, Hgf, and Hbegf (Fig. 5C). GSEA also revealed that MDMs have a higher ability to regulate endothelial cell proliferation than that of AMs (Fig. 5D). Based on the above results, we speculated that MDMs are pro-inflammatory in the early stage and pro-repairing in the later stage, so we analyzed the



Differences of Alveolar Macrophages

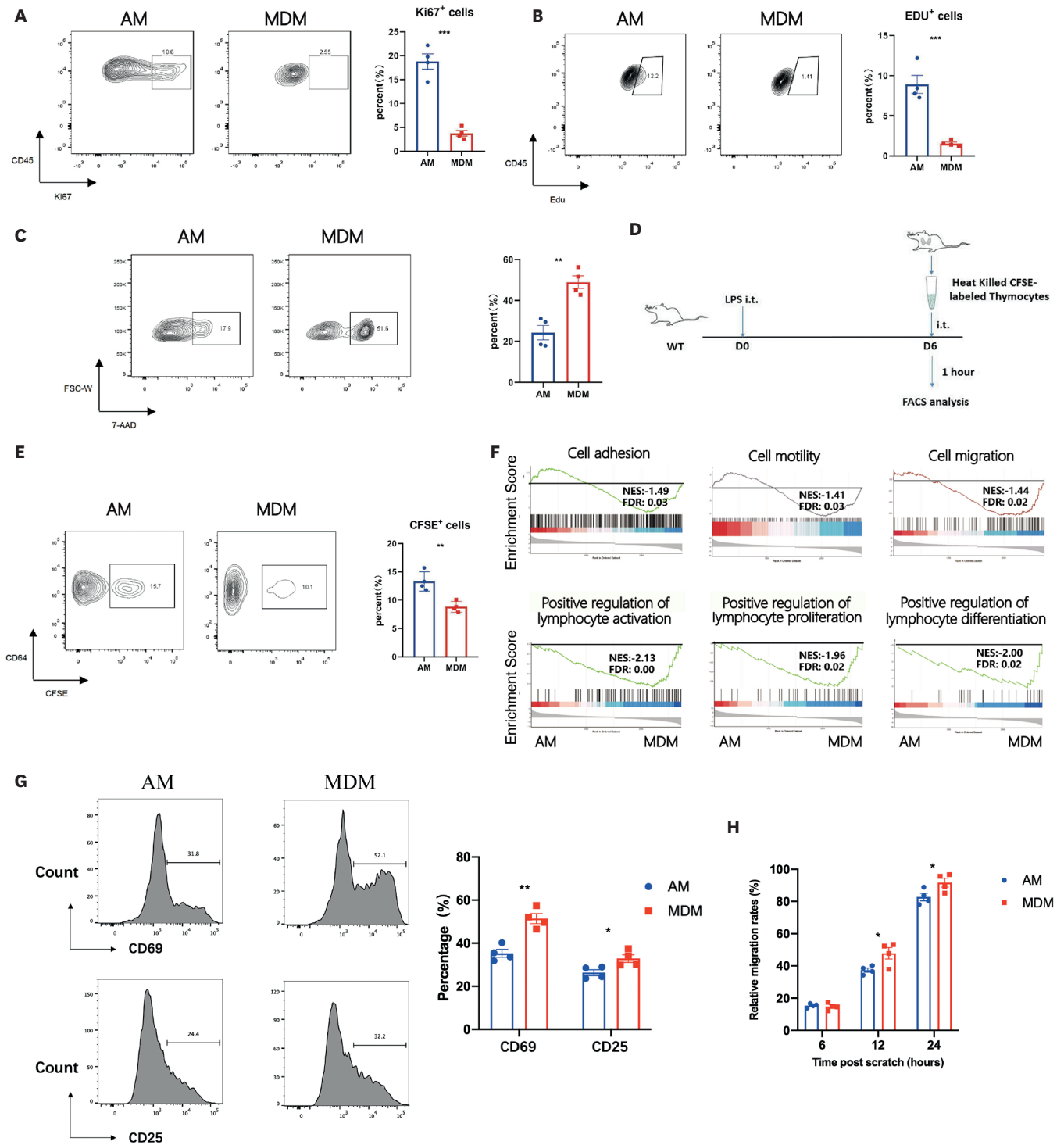


**Figure 4.** Viability and functional differences between AMs and MDMs. (A-C) Ki67, Edu and 7-AAD staining of AMs and MDMs on day 6 post LPS (n=4). Experiment was repeated three times. (D) Study design for phagocytosis analysis. (E) Percentage of CFSE+ cells of AMs and MDMs (n=4). Experiment was repeated three times. (F) GSEA of biological functions that represent cell adhesion, cell motility, cell migration, cell motility, cell migration, and positive regulation of lymphocyte activation, proliferation, and differentiation of AMs and MDMs. (G) Representative FACS plot and quantification of T cell activation marker CD25 and CD69 expression after co-cultured with AMs or MDMs overnight (n=4). (H) Migration rates of AMs and MDMs 6, 12, 24 h after scratch (n=4). \*p<0.05; \*\*p<0.01; \*\*\*p<0.001; \*\*\*\*p<0.0001.

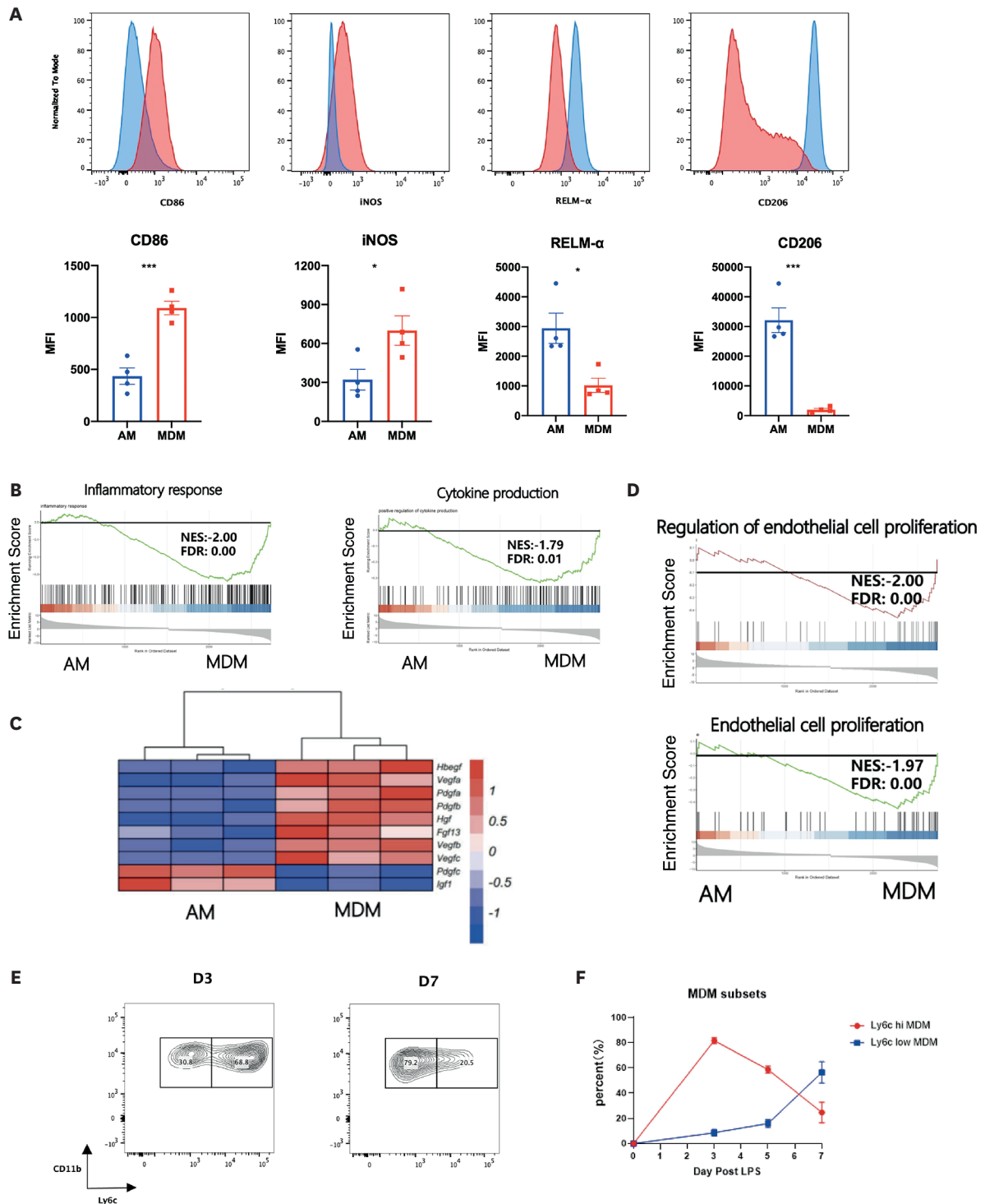


**Figure 5.** Phenotype differences of AMs and MDMs. (A) CD86, iNOS, RELM- $\alpha$  and CD206 expression levels of AMs and MDMs on day 6 post LPS (n=4). Experiment was repeated three times. (B) GSEA of inflammatory response and cytokine production functions of AMs and MDMs. (C) Heatmap of genes that represent tissue-repairing of AMs and MDMs. (D) GSEA of functions that represent regulating endothelial cell proliferation of AMs and MDMs. (E) Representative flow cytometry plots of Ly6c<sup>lo</sup> and Ly6c<sup>hi</sup> MDMs among Siglec-F<sup>+</sup> CD11b<sup>+</sup> MDMs from BALF on day 3 and day 7. (F) Percentages of Ly6c<sup>hi</sup> and Ly6c<sup>lo</sup> MDMs at different time points of ALI (n=3) per time point.

\*p<0.05; \*\*p<0.01; \*\*\*p<0.001; \*\*\*\*p<0.0001.

dynamic changes of Ly6c<sup>hi</sup> and Ly6c<sup>lo</sup> MDMs since Ly6c<sup>hi</sup> Cx3cr1<sup>lo</sup> MDMs are known as pro-inflammatory macrophages while Ly6c<sup>lo</sup> Cx3cr1<sup>hi</sup> MDMs are pro-resolving macrophages (20,21). As expected, the newly recruited macrophages were mainly Ly6c<sup>hi</sup> iMDMs and they gradually converted to Ly6c<sup>lo</sup> MDMs as inflammation subsides (Fig. 5E and F).

### iMDM significantly increased in BALF of severe COVID-19 patients

To verify that the characteristics of AMs and MDMs are also conserved in human, we analyzed a publicly available set of scRNA-seq data on BAL cells from patients with moderate or severe SARS-CoV-2 infection and healthy controls (GEO: GSE145926) (22). A total of 20 macrophages clusters were identified (Supplementary Fig. 2A) and the 20 clusters were assigned into 2 groups: AMs and MDMs according to the surface markers (Fig. 6A and B, Supplementary Fig. 2B). As expected, 2 groups of MDMs existed in the human lung: iMDMs and pro-repairing MDMs (pMDMs) (Fig. 6B). MDMs, especially iMDMs, were significantly increased in severe COVID-19 patients, suggesting that iMDMs have pro-inflammatory effects and may contribute to disease exacerbation (Fig. 6B). We then performed GO and KEGG pathway enrichment analyses on AMs and MDMs of severe COVID-19 patients. Unsurprisingly, MDMs are significantly enriched in inflammation-related pathways. (Fig. 6C). To verify the role of iMDM in lung injury, CCR2<sup>-/-</sup> mice were used to test the effect of blocking iMDM recruitment. On the third day after LPS injection, the number of MDMs in the BALF of CCR2<sup>-/-</sup> mice was significantly reduced (Fig. 6D), accompanied by a significant reduction in the degree of lung injury (Fig. 6E-G). Therefore, prolonged presence of iMDMs or failure to convert to pMDMs in a timely manner will worsen the disease.

## DISCUSSION

In ALI, lung macrophages are involved in the recovery from inflammation and tissue injury. In the past, AMs have been studied as a whole. However, recent studies have shown that AMs and MDMs are macrophages of different origins with different transcriptional and functional characteristics. However, apart from their origin, differences in their roles in the recovery period from lung injury remain unclear.

To study AMs and MDMs in lung injury, an LPS-induced mouse lung injury model was used and the transcriptional and functional characteristics of AMs and MDMs were analyzed. AMs and MDMs showed large differences at the transcription level. GO and KEGG pathway enrichment analyses indicated that AMs have high proliferation levels and lipid acid metabolism, while MDMs show stronger performance in inflammatory pathways and cytokine production. One study compared the metabolic characteristics of AMs and MDMs and found that MDMs increased glycolytic and arginine metabolism, whereas resident macrophages increased tricarboxylic acid cycle as well as amino acid and fatty acid metabolism (23). These results demonstrate the differences in the metabolism of AM and MDMs. However, the relationship between metabolic and functional differences remains unclear.

Survivability is an important difference between AMs and MDMs. Our study showed that AMs have stronger proliferative capacity and lower levels of cell death. This result is in line with the conclusions from some previous studies that AMs are long-lived macrophages that can multiply independent of monocytes, regardless of being in steady or infection states (15,16). MDMs are macrophages that inherit the characteristics of monocytes. They are short-lived cells with a low proliferation ability and a high percentage of death during the

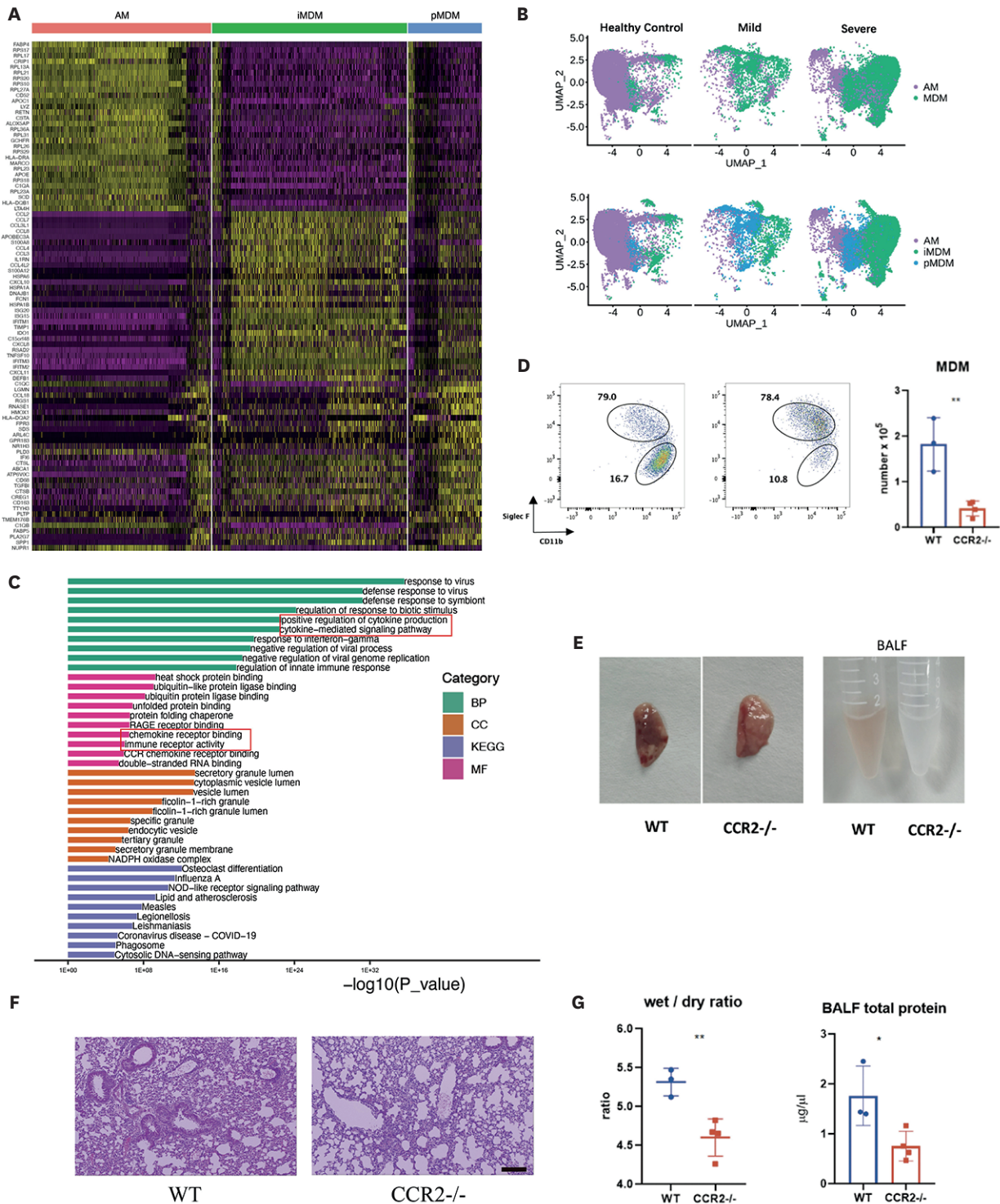


**Figure 6.** Analysis of scRNA-seq data on BAL cells from patients with SARS-CoV-2 infection. (A) The heatmaps of hierarchically clustered top 30 DEGs across 3 groups of macrophages. The gene names were listed to the left. (B) UMAP projection of 2 and 3 macrophage groups among controls (n=4) and patients (moderate, n=3; severe, n=6). (C) The GO and KEGG analysis of up-regulated DEGs showing some highlighted pathways in MDMs. (D) Representative flow cytometry plots of AMs (Siglec-F<sup>+</sup>CD11b<sup>+</sup>) and MDMs (Siglec-F<sup>+</sup>MerTK<sup>+</sup>) among CD64<sup>+</sup>MerTK<sup>+</sup> cells from BALF and quantification of cell numbers ( $\pm$ SEM) on the right (n=3-4). Experiment was repeated three times. (E) Lung tissue and BALF of WT and CCR2<sup>-/-</sup> mice on day3 post LPS. (F) Pulmonary pathology of WT and CCR2<sup>-/-</sup> mice on day 3 post LPS (bar=100  $\mu\text{m}$ ). (G, H): Lung wet/dry ratio and BALF total protein of WT and CCR2<sup>-/-</sup> mice on day 3 post LPS (n=3-4). Experiment was repeated three times. \*p<0.05; \*\*p<0.01.

recovery period. MDMs have been shown to undergo apoptosis during lung injury, and this process is determined by the death receptor Fas (24). Prevention of MDM apoptosis delays ALI resolution (24). Therefore, the number of AMs and MDMs are precisely controlled. The timely recovery of AMs and the decline in MDMs guarantees the resolution of inflammation. However, the precise mechanisms that regulate the number of AMs and MDMs remain unclear and require further exploration.

Our study also revealed differences in the phagocytic function of AMs and MDMs during recovery. The stronger phagocytosis of AMs during recovery is consistent with their ability to engulf surface proteins, bacteria, and dust in a steady state. Phagocytosis of apoptotic cells may promote the transition of macrophages (25,26) and enhance their proliferation ability (27); therefore, the high proliferation rate and rapid transition of AMs may also be related to phagocytosis. However, since the phagocytic capacity of macrophages is limited, it is unclear whether the weak phagocytic capacity of MDMs is related to their pre-phagocytosis of many apoptotic cells (28). In addition to their pro-repair function, MDMs are critical in activating adaptive immunity.

Macrophage phenotype transition occurs when the repair process starts (29,30). AMs and MDMs have been studied as a whole in the past, and thus, their respective phenotypic characteristics have been ignored. Our studies found that AMs display classical M2 markers, which is consistent with their repression phenotype in hemostasis. This may be related to their high level of proliferation for the reason that newly generated AMs exhibit the repression phenotype (16). Therefore, AMs may be critical in mediating the resolution of inflammation. In the acute inflammation phase, MDMs have been demonstrated to produce higher levels of IL-1 $\beta$ , IL-6, IL-12p70, keratinocyte chemokine, and IL-10 than those by AMs (23). During the recovery period, MDMs also expressed high levels of pro-inflammatory genes, such as Il6, Tnf, and Nos2. MDMs also exhibited higher expression of M1 markers than that by AMs, indicating that MDMs may be the main source of cytokine storm and cause tissue injury in ALI (31-33). Paradoxically, MDMs show a stronger ability to repair tissues, despite their M1 phenotype. These results suggest that there may be distinct sub-populations of MDMs with a constant, dynamic change. The transition from iMDMs to pMDMs is an important condition for tissue damage repair. However, the long-term existence of pMDMs may contribute to fibrosis (34). Therefore, timely death of MDMs is an important part of recovery. Our study showed that the increase of iMDMs may contribute to worsening condition of lung infection and blocking the recruitment of iMDMs may reduce lung injury. However, considering the function of defending pathogens and activating T and B cells of MDMs, totally blocking the recruitment of MDMs may be not the best choice. The intervention of macrophages should focus on increasing the number of AMs, promoting the death of excess iMDMs or promoting conversion of iMDMs to pMDMs.

In summary, this study compared the transcriptional and functional differences of AMs and MDMs during ALI recovery. The results of this study found that AMs are highly proliferating macrophages with a repression phenotype and high phagocytic ability, while MDMs are the main pro-repairing macrophages with a paradoxical phenotype and undergo a large amount of cell death during the recovery phase. These results provide clues for future research on the mechanisms and interventions for lung injury.

## ACKNOWLEDGEMENTS

This study was supported by National Natural Science Foundation of China (NSFC) (82172109) and Youth Talent Fund Project (2019BJRC03).

## SUPPLEMENTARY MATERIALS

### Supplementary Figure 1

Cluster dendrogram of AMs and MDMs gene expression.

[Click here to view](#)

### Supplementary Figure 2

(A) The heatmap of 13 markers across 20 clusters of macrophages. The gene names were listed to the left. (B) UMAP plots showing the expression of several markers on BALF macrophages.

[Click here to view](#)

## REFERENCES

1. Meyer NJ, Gattinoni L, Calfee CS. Acute respiratory distress syndrome. *Lancet* 2021;398:622-637.  
[PUBMED](#) | [CROSSREF](#)
2. Soni S, Wilson MR, O'Dea KP, Yoshida M, Katbeh U, Woods SJ, Takata M. Alveolar macrophage-derived microvesicles mediate acute lung injury. *Thorax* 2016;71:1020-1029.  
[PUBMED](#) | [CROSSREF](#)
3. Aggarwal NR, King LS, D'Alessio FR. Diverse macrophage populations mediate acute lung inflammation and resolution. *Am J Physiol Lung Cell Mol Physiol* 2014;306:L709-L725.  
[PUBMED](#) | [CROSSREF](#)
4. Hou F, Xiao K, Tang L, Xie L. Diversity of macrophages in lung homeostasis and diseases. *Front Immunol* 2021;12:753940.  
[PUBMED](#) | [CROSSREF](#)
5. Gomez Perdiguero E, Klapproth K, Schulz C, Busch K, Azzoni E, Crozet L, Garner H, Trouillet C, de Bruijn MF, Geissmann F, et al. Tissue-resident macrophages originate from yolk-sac-derived erythro-myeloid progenitors. *Nature* 2015;518:547-551.  
[PUBMED](#) | [CROSSREF](#)
6. Guilliams M, De Klerk I, Henri S, Post S, Vanhoutte L, De Prijck S, Deswarte K, Malissen B, Hammad H, Lambrecht BN. Alveolar macrophages develop from fetal monocytes that differentiate into long-lived cells in the first week of life via GM-CSF. *J Exp Med* 2013;210:1977-1992.  
[PUBMED](#) | [CROSSREF](#)
7. Broug-Holub E, Toews GB, van Iwaarden JF, Strieter RM, Kunkel SL, Paine R 3rd, Standiford TJ. Alveolar macrophages are required for protective pulmonary defenses in murine *Klebsiella pneumoniae*: elimination of alveolar macrophages increases neutrophil recruitment but decreases bacterial clearance and survival. *Infect Immun* 1997;65:1139-1146.  
[PUBMED](#) | [CROSSREF](#)
8. Byrne AJ, Mathie SA, Gregory LG, Lloyd CM. Pulmonary macrophages: key players in the innate defence of the airways. *Thorax* 2015;70:1189-1196.  
[PUBMED](#) | [CROSSREF](#)
9. Herold S, Mayer K, Lohmeyer J. Acute lung injury: how macrophages orchestrate resolution of inflammation and tissue repair. *Front Immunol* 2011;2:65.  
[PUBMED](#) | [CROSSREF](#)

10. Watanabe S, Alexander M, Misharin AV, Budinger GR. The role of macrophages in the resolution of inflammation. *J Clin Invest* 2019;129:2619-2628.  
[PUBMED](#) | [CROSSREF](#)
11. Grégoire M, Uhel F, Lesouhaitier M, Gacouin A, Guirriec M, Mourcin F, Dumontet E, Chalin A, Samson M, Berthelot LL, et al. Impaired efferocytosis and neutrophil extracellular trap clearance by macrophages in ARDS. *Eur Respir J* 2018;52:1702590.  
[PUBMED](#) | [CROSSREF](#)
12. Doran AC, Yurdagul A Jr, Tabas I. Efferocytosis in health and disease. *Nat Rev Immunol* 2020;20:254-267.  
[PUBMED](#) | [CROSSREF](#)
13. Aegerter H, Kulikauskaite J, Crotta S, Patel H, Kelly G, Hessel EM, Mack M, Beinke S, Wack A. Influenza-induced monocyte-derived alveolar macrophages confer prolonged antibacterial protection. *Nat Immunol* 2020;21:145-157.  
[PUBMED](#) | [CROSSREF](#)
14. Svedberg FR, Brown SL, Krauss MZ, Campbell L, Sharpe C, Clausen M, Howell GJ, Clark H, Madsen J, Evans CM, et al. The lung environment controls alveolar macrophage metabolism and responsiveness in type 2 inflammation. *Nat Immunol* 2019;20:571-580.  
[PUBMED](#) | [CROSSREF](#)
15. Hashimoto D, Chow A, Noizat C, Teo P, Beasley MB, Leboeuf M, Becker CD, See P, Price J, Lucas D, et al. Tissue-resident macrophages self-maintain locally throughout adult life with minimal contribution from circulating monocytes. *Immunity* 2013;38:792-804.  
[PUBMED](#) | [CROSSREF](#)
16. Zhu B, Wu Y, Huang S, Zhang R, Son YM, Li C, Cheon IS, Gao X, Wang M, Chen Y, et al. Uncoupling of macrophage inflammation from self-renewal modulates host recovery from respiratory viral infection. *Immunity* 2021;54:1200-1218.e9.  
[PUBMED](#) | [CROSSREF](#)
17. Neupane AS, Willson M, Chojnacki AK, Vargas E Silva Castanheira F, Morehouse C, Carestia A, Keller AE, Peiseler M, DiGiandomenico A, Kelly MM, et al. Patrolling alveolar macrophages conceal bacteria from the immune system to maintain homeostasis. *Cell* 2020;183:110-125.e11.  
[PUBMED](#) | [CROSSREF](#)
18. Wynn TA, Vannella KM. Macrophages in tissue repair, regeneration, and fibrosis. *Immunity* 2016;44:450-462.  
[PUBMED](#) | [CROSSREF](#)
19. Ortega-Gómez A, Perretti M, Soehnlein O. Resolution of inflammation: an integrated view. *EMBO Mol Med* 2013;5:661-674.  
[PUBMED](#) | [CROSSREF](#)
20. Dal-Secco D, Wang J, Zeng Z, Kolaczowska E, Wong CH, Petri B, Ransohoff RM, Charo IF, Jenne CN, Kubes P. A dynamic spectrum of monocytes arising from the in situ reprogramming of CCR2+ monocytes at a site of sterile injury. *J Exp Med* 2015;212:447-456.  
[PUBMED](#) | [CROSSREF](#)
21. Yang W, Tao Y, Wu Y, Zhao X, Ye W, Zhao D, Fu L, Tian C, Yang J, He F, et al. Neutrophils promote the development of reparative macrophages mediated by ROS to orchestrate liver repair. *Nat Commun* 2019;10:1076.  
[PUBMED](#) | [CROSSREF](#)
22. Liao M, Liu Y, Yuan J, Wen Y, Xu G, Zhao J, Cheng L, Li J, Wang X, Wang F, et al. Single-cell landscape of bronchoalveolar immune cells in patients with COVID-19. *Nat Med* 2020;26:842-844.  
[PUBMED](#) | [CROSSREF](#)
23. Mould KJ, Barthel L, Mohning MP, Thomas SM, McCubbrey AL, Danhorn T, Leach SM, Fingerlin TE, O'Connor BP, Reisz JA, et al. Cell origin dictates programming of resident versus recruited macrophages during acute lung injury. *Am J Respir Cell Mol Biol* 2017;57:294-306.  
[PUBMED](#) | [CROSSREF](#)
24. Janssen WJ, Barthel L, Muldrow A, Oberley-Deegan RE, Kearns MT, Jakubzick C, Henson PM. Fas determines differential fates of resident and recruited macrophages during resolution of acute lung injury. *Am J Respir Crit Care Med* 2011;184:547-560.  
[PUBMED](#) | [CROSSREF](#)
25. Huynh ML, Fadok VA, Henson PM. Phosphatidylserine-dependent ingestion of apoptotic cells promotes TGF-beta1 secretion and the resolution of inflammation. *J Clin Invest* 2002;109:41-50.  
[PUBMED](#) | [CROSSREF](#)
26. Fadok VA, Bratton DL, Konowal A, Freed PW, Westcott JY, Henson PM. Macrophages that have ingested apoptotic cells *in vitro* inhibit proinflammatory cytokine production through autocrine/paracrine mechanisms involving TGF-beta, PGE2, and PAF. *J Clin Invest* 1998;101:890-898.  
[PUBMED](#) | [CROSSREF](#)

27. Gerlach BD, Ampomah PB, Yurdagül A Jr, Liu C, Lauring MC, Wang X, Kasikara C, Kong N, Shi J, Tao W, et al. Efferocytosis induces macrophage proliferation to help resolve tissue injury. *Cell Metab* 2021;33:2445-2463.e8.  
[PUBMED](#) | [CROSSREF](#)
28. Schif-Zuck S, Gross N, Assi S, Rostoker R, Serhan CN, Ariel A. Saturated-efferocytosis generates pro-resolving CD11b low macrophages: modulation by resolvins and glucocorticoids. *Eur J Immunol* 2011;41:366-379.  
[PUBMED](#) | [CROSSREF](#)
29. Van Dyken SJ, Locksley RM. Interleukin-4- and interleukin-13-mediated alternatively activated macrophages: roles in homeostasis and disease. *Annu Rev Immunol* 2013;31:317-343.  
[PUBMED](#) | [CROSSREF](#)
30. Minutti CM, Jackson-Jones LH, García-Fojeda B, Knipper JA, Sutherland TE, Logan N, Ringqvist E, Guillamat-Prats R, Ferenbach DA, Artigas A, et al. Local amplifiers of IL-4R $\alpha$ -mediated macrophage activation promote repair in lung and liver. *Science* 2017;356:1076-1080.  
[PUBMED](#) | [CROSSREF](#)
31. Dhaliwal K, Scholefield E, Ferenbach D, Gibbons M, Duffin R, Dorward DA, Morris AC, Humphries D, MacKinnon A, Wilkinson TS, et al. Monocytes control second-phase neutrophil emigration in established lipopolysaccharide-induced murine lung injury. *Am J Respir Crit Care Med* 2012;186:514-524.  
[PUBMED](#) | [CROSSREF](#)
32. Junqueira C, Crespo Â, Ranjbar S, de Lacerda LB, Lewandrowski M, Ingber J, Parry B, Ravid S, Clark S, Schrimpf MR, et al. Fc $\gamma$ R-mediated SARS-CoV-2 infection of monocytes activates inflammation. *Nature* 2022;606:576-584. ; Online ahead of print.  
[PUBMED](#) | [CROSSREF](#)
33. Merad M, Martin JC. Pathological inflammation in patients with COVID-19: a key role for monocytes and macrophages. *Nat Rev Immunol* 2020;20:355-362.  
[PUBMED](#) | [CROSSREF](#)
34. Misharin AV, Morales-Nebreda L, Reyfman PA, Cuda CM, Walter JM, McQuattie-Pimentel AC, Chen CI, Anekalla KR, Joshi N, Williams KJ, et al. Monocyte-derived alveolar macrophages drive lung fibrosis and persist in the lung over the life span. *J Exp Med* 2017;214:2387-2404.  
[PUBMED](#) | [CROSSREF](#)